

# Numerical investigation of fluid-structure interaction in a model of solid propellant motors

*C. Rey\*, V. Froment\*, M.-P. Errera\*\*, B.Truffart\*\*\*, A.Langlois\*\*\**

*\*Snecma Propulsion Solide, SAFRAN Group*

*Les cinq chemins, 33187 Le Haillan, France*

*\*\*ONERA*

*29 avenue de la Division Leclerc, 92322 Châtillon Cedex, France*

*\*\*\*MSC.Software France*

*6-8 rue Ambroise Croizat, ZA Les Glaises, 91120 Palaiseau Cedex*

## Abstract

The coupling Fluid-Structure Interaction (FSI) procedure developed by Snecma Propulsion Solide, SAFRAN Group jointly with ONERA and MSC.Software is described in this paper. Numerical results are first confronted to experimental data on a reference test case. A good agreement that validates the coupling methodology is obtained. Then a simplified small scale configuration of a segmented Solid Rocket Motor is computed. The comparison between uncoupled and coupled simulations, still under investigation, exhibits a frequency shift in the flow acoustic coupling. Hence, in this particular configuration, FSI phenomena may alter the aeroacoustic instability.

## Introduction

Numerical simulation of Solid Rocket Motors (SRMs) is a complicated and multi-physics problem. Numerous physical fields such as fluid dynamics of reacting and multiphase flows, structural analysis with visco-elastic behaviour, combustion of solid propellant, heat transfer and radiation are closely connected with each other. In order to improve the analysis and optimization of SRMs design, multidisciplinary simulations have become a strong industrial requirement.

Snecma Propulsion Solide, SAFRAN Group has been developing coupled simulations for three years, jointly with ONERA and MSC.Software. Up to now, two kinds of multiphysics problems were addressed: fluid-solid thermal coupling and Fluid-Structure Interactions (FSI). In this paper one focuses only on the latter interaction. The coupling FSI strategy described in the first part of this article is used to improve the physical understanding of the two following topics:

- ü the ignition of SRMs, with the fluid flow and the structural displacements closely coupled during the first milliseconds.
- ü the pressure and thrust oscillations in segmented SRMs.

In the present paper, only this last application is investigated. Such oscillations which could damage the payload are commonly described as a feedback loop between longitudinal acoustic modes of the combustion chamber and hydrodynamic instabilities of shear regions of the flow <sup>[1] [2] [3]</sup>. Two mechanisms of vortex shedding are usually described in the literature:

- ü Obstacle Vortex Shedding (VSO) generated at the edge of the Frontal Thermal Protection (PTF) protruding into the flow due to the regression of the burning surface,
- ü Parietal Vortex Shedding<sup>[4]</sup> (VSP) originating from a natural instability of the bending flow resulting from the propellant combustion.

FSI phenomena could alter this aeroacoustic instability either through the vibrations of the deformable PTF or through the structural modes of the motor. Figure 1 describes a possible feedback loop of the relevant phenomena involved during the transient regime of segmented SRMs.

Our purpose was first to validate the FSI approach in the context of highly transient compressible flows. The comparison between experimental data<sup>[4]</sup> and numerical results are given in the 2<sup>nd</sup> part of this article. Then a simplified small scale configuration of the Ariane 5 SRM is computed. This configuration allows us to study the feedback loop between the acoustics of the chamber, Obstacle Vortex Shedding occurring at the edge of the PTF and the PTF vibrations. Results of this simulation and comparison to an uncoupled one are presented in section 3.

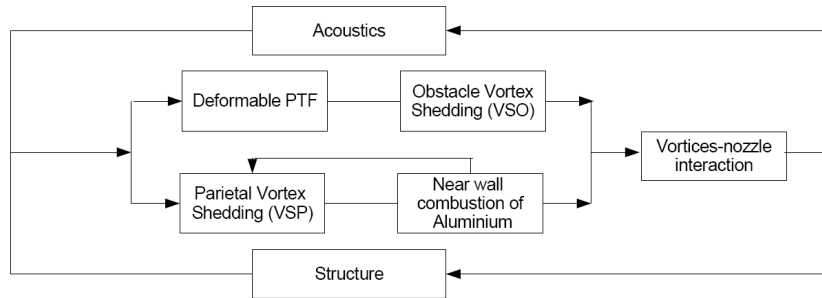


Figure 1 : Possible feedback loop during the transient regime of SRMs.

## 1. Coupling strategy

### 1.1 Coupling procedure

In the weakly coupled approach used here, the FSI is achieved by partitioning the problem into fluid and solid parts solved separately with boundary conditions calculated by the other part. This leads to a sequential treatment of the fluid and solid domains that can be seen as a Conventional Serial Staggered (CSS) procedure<sup>[6]</sup>. In this approach, the structural and fluid are calculated independently from each other respectively with MSC.MARC and MSD. The transfer of the physical data is performed by the coupling library MpCCI. Figure 2 shows the sequence of iteration steps. It starts with the calculation of the aerodynamic field by an unsteady procedure (path 1). The resulting pressure distribution  $P$  is transferred to the finite element nodes (path 2). Using this new interface conditions the structural code computes the deformation  $U$  of the structure (path 3). The resulting displacements modify the fluid surface grid and consequently change the boundary conditions (path 4) but also the entire grid in the fluid domain in the next step (path 5).

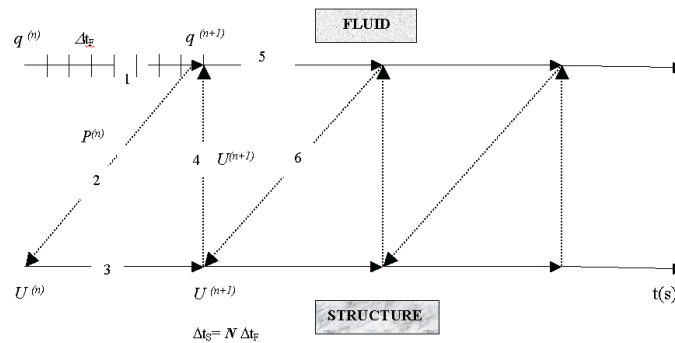


Figure 2 : FSI numerical procedure

### 1.2 The Structural Solver : MSC.MARC

MSC.MARC is a general-purpose implicit nonlinear finite element analysis software that can simulate static and dynamic structural problems for a wide range of design and manufacturing applications. In this paper, direct integration, based on a Newmark-beta scheme, is used to solve the equations of motion of the structural part.

This code includes a comprehensive finite element library (solid or shell elements, linear or quadratic) and also provides an extensive library of material models.

Mooney-Rivlin formulations are used for handling (quasi)incompressible material behaviour, as well as a generalized Maxwell model (based on hereditary integral) for viscoelastic behaviour (section 3).

### 1.3 The Flow Solver : MSD

The computer code in the fluid, called MSD, has been developed since the mid 1980s at ONERA<sup>[7][8]</sup>. This code can compute turbulent reactive flows of realistic aerospace configurations and is widely used in a great variety of scientific and engineering problems : turbojet, ramjet, liquid and solid propellant rocket.

MSD is a 3D finite-volume structured code. The governing equations, written in the conservative form, are the Navier-Stokes equations.

In this paper, the equations are solved using a second-order upwind discretization scheme based on Roe's flux difference splitting. The time integration is obtained by an implicit factored method. Various turbulence models of different complexity are available in this code. In the coupled computation described in section 3, the main flow equations are closed using the two equations k-l turbulence model<sup>[9]</sup> with wall functions. In the test case presented in section 2, the fluid flow is assumed to be laminar.

#### 1.4 The coupling library : MpCCI

The transfer of the physical data between the structured mesh for the fluid code and the unstructured mesh for the structural solver is performed through the MpCCI (Mesh-based parallel Code Coupling Interface) library, developed by Fraunhofer Institute SCAI, Germany<sup>[10]</sup>. Each code uses its own grid generated independently and the user only specifies the coupling surfaces, namely the basic geometries of the coupling surfaces and the transferred values. MpCCI's task is to calculate the neighborhood relations and to transfer the coupling values across the fluid-structure interface. Consequently, it is responsible for transferring data at the fluid-solid interface, where the two grids are non-matching.

## 2. Numerical simulation of a validation test case

### 2.1 Choice of the FSI reference case

In this part, our goal is to compare the coupling strategy described in section 1 with an unsteady FSI problem. Such a constraint is very restrictive because of the lack of reference cases available to validate FSI in the context of highly transient compressible flows. The experimental device proposed and designed by J. Giordano<sup>[4]</sup> is studied. It is constituted of a deforming cantilever steel panel submitted to a shock tube flow. The base on which the deformable panel is fixed is assumed to be infinitely rigid. A close-up view of this experimental set-up is given in Figure 3.

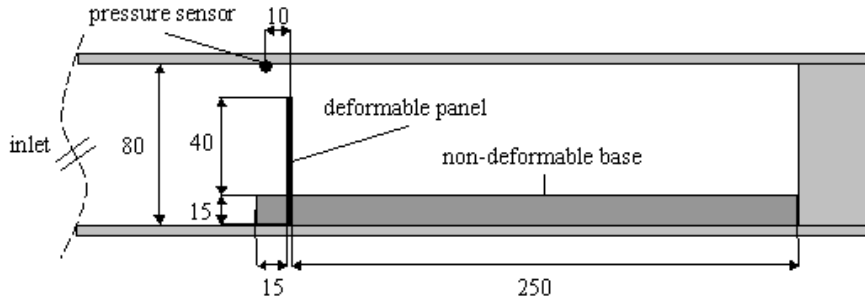


Figure 3 : Experimental set-up. Dimensions in mm.

The panel is deformed by the pressure gradient induced by shock waves and, in response, its motion alters the fluid flow. Two types of experimental diagnostics<sup>[4]</sup> are available to validate the numerical results : the panel displacement and pressure evolution at the sensor position.

### 2.2 Numerical Model

The coupled simulation is performed for a steel panel (Linear elastic, isotropic material : Young Modulus  $E=220$  GPa, density  $\rho = 7600$  kg/m<sup>3</sup>) with length equal to 40 mm. Its thickness is 1 mm. No material damping is assumed. The shock wave moves from the inlet boundary condition at Mach number of 1.2 in air at rest ( $1.0 \cdot 10^5$  Pa and 293 K). Thus the flow has to be considered as compressible. Turbulence will be neglected because of the short experimental durations involved (of the order of a few ms).

The whole shock tube geometry has not been modeled. The fluid flow mesh plotted on Figure 4 is composed of 120000 cells. The inlet boundary condition is such that waves can pass through it without any reflection. Note that the transversal dimension of the first fluid cell next to the deformable panel is equal to 0.05 mm.

The coupling time step is taken to be equal to  $10 \mu\text{s}$  which is more than 100 times smaller than the experimental structural period. Hence one can assume the coupled dynamics to be respected and also the Geometric Conservation Law to be checked<sup>[13]</sup>.

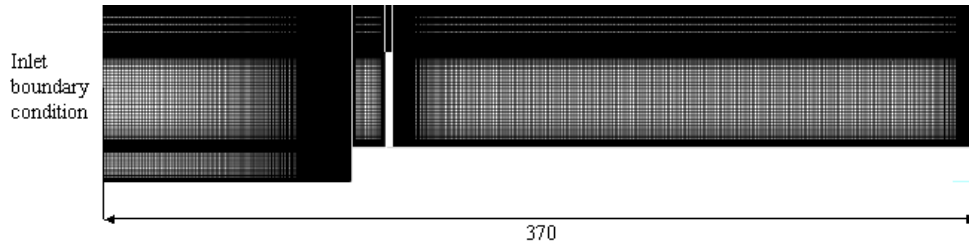


Figure 4 : Fluid flow mesh. Dimensions in mm.

### 2.3 Numerical results and comparison to experimental data

The description of the physical phenomena occurring into the shock tube are discussed in details by J. Giordano<sup>[4]</sup>. One focuses here only on the quantitative comparison between our numerical results and the experimental data<sup>[4]</sup>. Numerical schlieren images are given in Figure 5 in order to make easier the understanding of the time evolution of pressure. This evolution at the probe position is plotted on Figure 6. Time  $t = 0.0s$  coincides with the arrival of the incident shock wave at that position. When this shock wave interacts with the cantilever panel, reflected and transmitted shock waves are created. In the simulation, the reflected shock wave passes through the sensor position at  $t = 110 \mu s$  and the reflected transmitted shock wave arrives at  $t = 1.44 ms$ . One can notice that the time evolution of the numerical results agrees well with the experimental ones<sup>[4]</sup>.

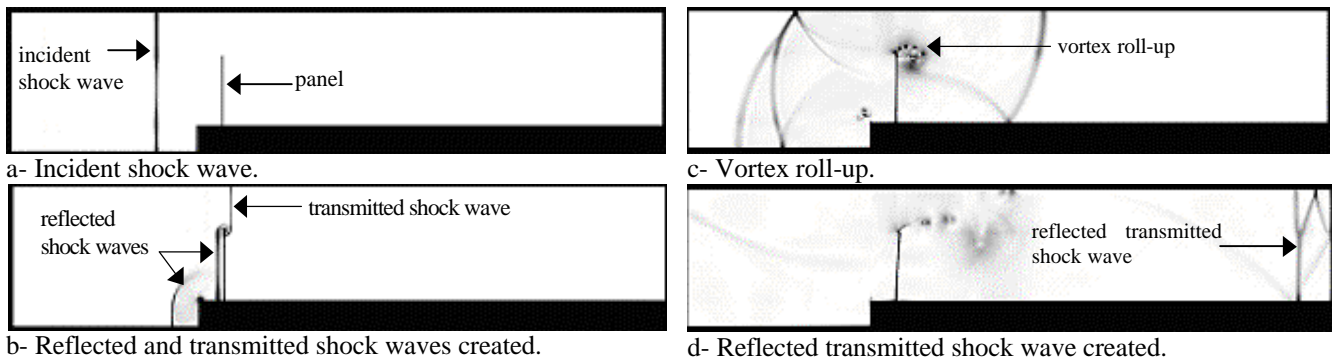


Figure 5 : Numerical Schlieren.

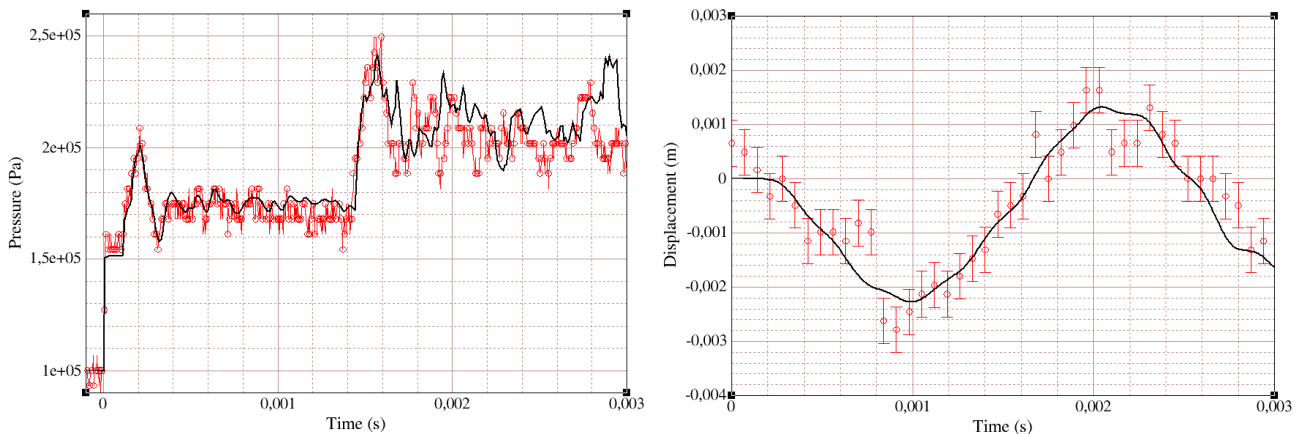


Figure 6 : Time evolution of pressure (left) and of panel displacement (right). thick line : numerical results, red circles : experimental result<sup>[4]</sup>.

Moreover, up to 2 ms, the coupling method provides pressure amplitudes that are very close to the experiment. For  $t > 2ms$ , the numerical results cannot be compared any more with the experimental ones. The reflection of the expansion waves is indeed not taken into account into the simulation because of the non reflecting inlet boundary condition.

The time evolution of displacement is plotted on Figure 6. As far as the period of the movement is concerned, results of the simulation and experiment are close. Besides, the maximum displacement is well predicted by the simulation.

All the comparisons show a good agreement between the numerical results and the experimental data<sup>[4]</sup> in this configuration that involves highly transient phenomena. This constitutes a first step in the validation process of the coupling method. In the future, one plans to simulate new test cases involving stronger coupling phenomena in order to assess the domain of validity of this coupling procedure.

### 3. Application to a simplified small scale configuration of the Ariane5 SRM

#### 3.1 Choice of the geometric configuration

Pressure and thrust oscillations in segmented SRMs is a multi-physics problem, involving more particularly Fluid-Structure Interaction<sup>[11]</sup>. In a first attempt to assess the importance of FSI phenomena, one simulates a simplified small scale configuration of the Ariane5 SRM using the coupling methodology described above. The studied geometry is similar to the one of the VALDO<sup>[12]</sup> experimental facility designed by ONERA. It is constituted of a cylindrical chamber (length= $L=504\text{mm}$ , radius= $30\text{mm}$ ) with exit nozzle. An obstacle which stands for the Frontal Thermal Protection (PTF) is placed at  $336\text{mm}$  ( $2/3*L$ ) from the head (Figure 7).

The aerodynamic phenomena involved in the Ariane 5 SRM and VALDO experiments are simplified in the simulation performed here. In particular, injection at the wall and the related Parietal Vortex Shedding (VSP) are not taken into account. Indeed one focuses in this simulation only on the possible feedback loop between the longitudinal acoustic mode of the chamber, Obstacle Vortex Shedding (VSO) occurring at the edge of the PTF and the PTF vibrations (Figure 8).

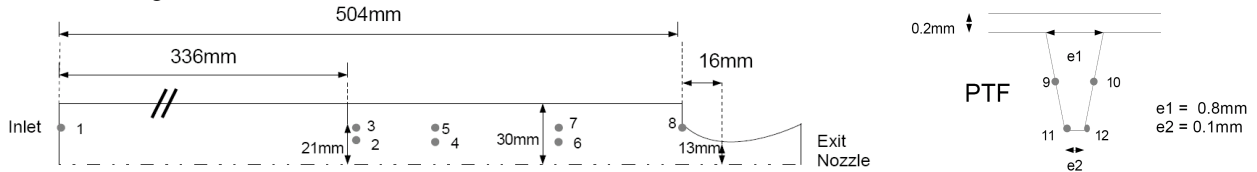


Figure 7 : left) General set-up of the VALDO geometry . right) Close-up view of the PTF geometry.

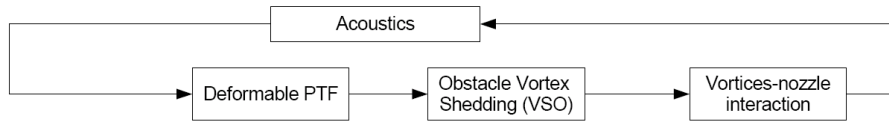


Figure 8 : Simplified feedback loop investigated.

#### 3.2 Numerical model

The combustion chamber is filled with dinitrogen ( $\text{N}_2$ ) at rest ( $P_{\text{init}} = 0.1\text{bar}$ ,  $T_{\text{init}} = 298\text{K}$ ). Dinitrogen is also injected at the inlet boundary condition at a temperature of  $298\text{K}$  with a mass flow-rate of  $90\text{kg/s}$  which is such that an average chamber pressure of  $2\text{bar}$  is reached. The mass flux is prescribed with a ramp that allows not to create a violent transient in the flow at the beginning. The static pressure imposed at the exit of the nozzle is  $0.1\text{bar}$ . The flow is assumed to be turbulent and a two equations k- $\epsilon$  model with wall functions is used. A low rate of turbulence is injected at the inflow ( $l = 10e-4\text{m}$  and  $\tau = u'/u = 0.005$ ).

Both assumptions of quasi-incompressible and time-dependent (viscoelastic) behaviour are made for the PTF (elastomeric material,  $\rho = 1100\text{kg/m}^3$ ). Hence, the Mooney formulation (within a Total Lagrangian framework) is used in conjunction with a stress relaxation function, that is provided through the terms of a Prony series.

The fluid and structural meshes are respectively constituted of 18685 cells and 2011 nodes. The simulation is carried out on 100ms in order to reach the mean pressure of  $2\text{bar}$  and have a long-enough quasi-stationary period of simulation to perform a frequency analysis. Numerical pressure sensors are placed as plotted on Figure 7.

#### 3.3 Numerical results

Two different simulations are performed. The first one is a purely aerodynamical uncoupled simulation while the second one is a fully coupled fluid-structure calculation.

The fluid flow solver MSD is used to compute the uncoupled CFD simulation. The PTF is assumed to be non deformable with a geometry identical to the mean deformed one obtained from the coupled simulation (see below and Figure 14.b). After a transient ramp-up regime, the pressure evolution becomes quasi-periodical with a mean value of  $2\text{bar}$  as plotted on Figure 9. A Fourier analysis performed between 80 and 100 ms gives a frequency peak of

650 Hz which corresponds to the 2<sup>nd</sup> longitudinal acoustic mode (2L) frequency. A possible flow acoustic coupling with 2 vortices lying between the PTF and the nozzle is observed in this uncoupled configuration. Rockwell expressed it with the following formula<sup>[14]</sup>:  $mT = \frac{l}{kU_{jet}} + \frac{l}{c - U_{jet}} + \Delta t$ , where  $T$  is the period of obstacle vortex shedding,  $l$  is the obstacle-nozzle distance,  $U_{jet}$  is the mean velocity of the jet generated at the inhibitor,  $m$  is the number of vortices lying between the obstacle and the nozzle,  $kU_{jet}$  is the convection velocity of the vortices and  $\Delta t$  is a small time increment that represents the duration of creation of the vortices and that can be expressed as  $\alpha T$ . The uncoupled simulation provides the following values:  $U_{jet} = 90\text{m/s}$ ,  $kU_{jet} = 63\text{m/s}$ ,  $c = 322\text{m/s}$ ,  $l = 0.164\text{m}$ . Besides for the application to the SRM P230 booster, experimental results at full scale give  $\alpha = 0.1$ <sup>[15]</sup>. Applying Rockwell’s formula with  $m=2$ , one finds  $f=574$  Hz. Considering the uncertainties of the parameters  $U_{jet}$ ,  $kU_{jet}$  and  $\alpha$ , this frequency is found to be close to the observed one.

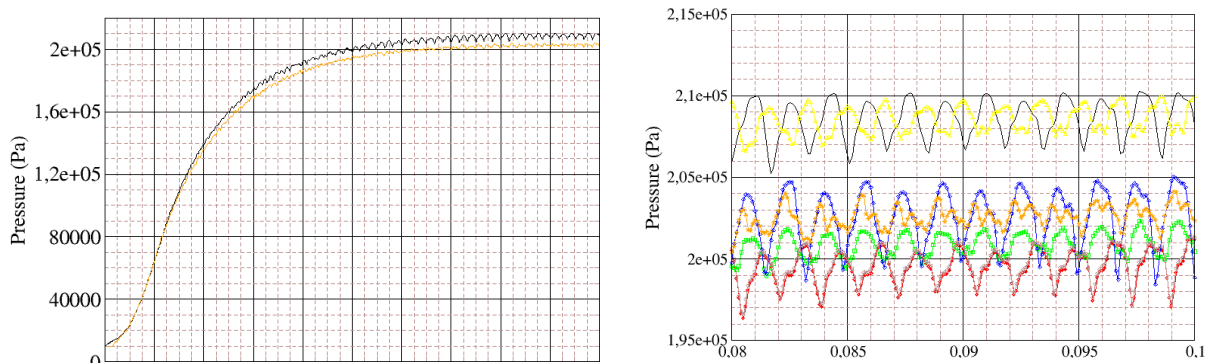


Figure 9 : Pressure evolution for the uncoupled calculation. a) complete evolution for sensors 1 (black) and 7 (orange). b) 80-100ms evolution for sensors 1 (black), 3 (red, circle), 5 (green, square), 7 (orange, star), 8 (blue, diamond), 9 (yellow, triangle up) and 10 (brown, triangle left).

To determine the influence of FSI phenomena, a coupled simulation is performed with the coupling methodology. The initial geometry of the obstacle ( $t=0.0\text{s}$ ) is the non-deformed one. Pressure records and PTF displacements are plotted on Figure 10 and Figure 11. The time evolution of these variables becomes quasi-periodical after 80 ms. The mean axial and radial displacements of the inhibitor are respectively 3.75 mm and 1.05 mm (Figure 14). These values determine the mean deformed geometry taken into account in the uncoupled simulation. During the quasi-periodical regime, the pressure and displacements are found to oscillate at a frequency of 1200 Hz. This value corresponds to the 4<sup>th</sup> longitudinal acoustic mode (4L) which mode shape is plotted on Figure 12. The application of Rockwell’s formula with the following values:  $U_{jet} = 80\text{m/s}$ ,  $kU_{jet} = 57\text{m/s}$ ,  $c = 322\text{m/s}$ ,  $l = 0.164\text{m}$  and  $\alpha = 0.1$  gives a vortex shedding frequency equal to  $f = 1100\text{Hz}$  with  $m=4$ . Hence a flow acoustic coupling with 4 vortices (Figure 13) lying between the obstacle and the nozzle is possibly observed in the coupled configuration.

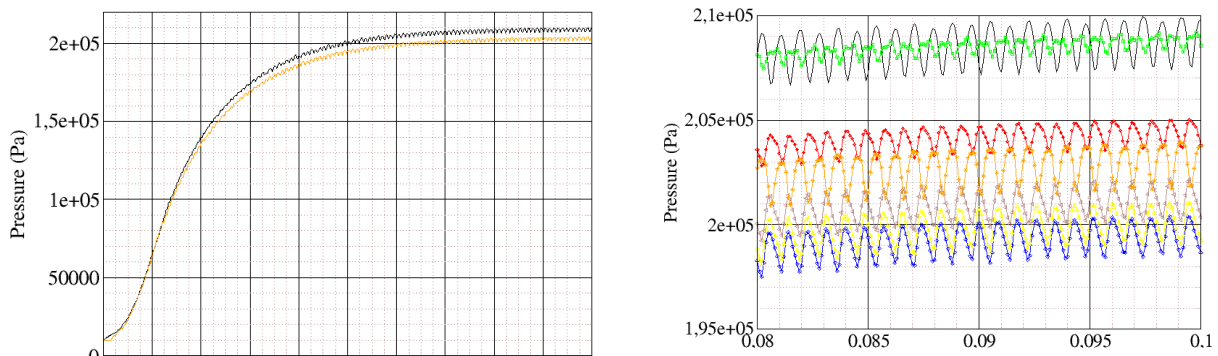


Figure 10 : Pressure evolution for the coupled calculation. a) complete evolution for sensors 1 (black) and 7 (orange). b) 80-100ms evolution for sensors 1 (black), 3 (red, circle), 5 (green, square), 7 (orange, star), 8 (blue, diamond), 9 (yellow, triangle up) and 10 (brown, triangle left).

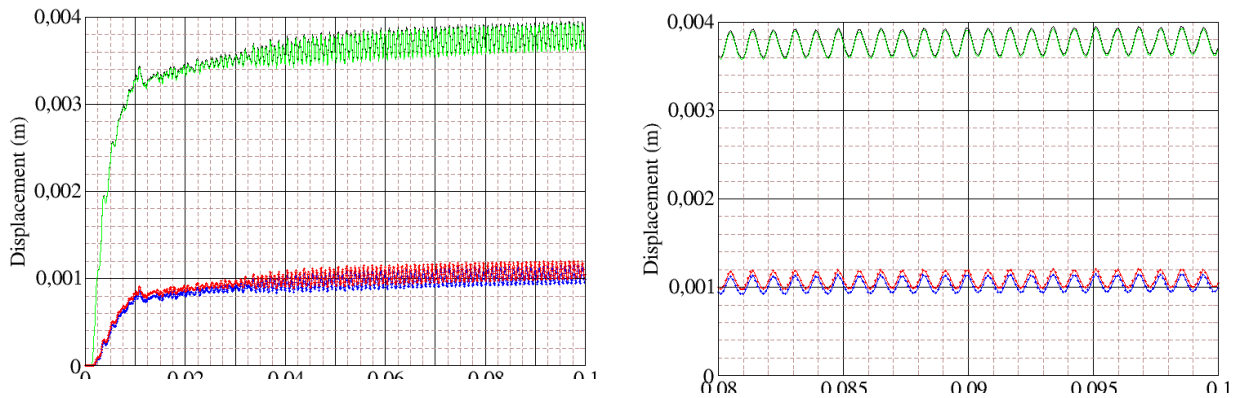


Figure 11 : Displacement of the PTF on sensors 11 (axial in black, radial in blue circle) and 12 (axial in green, radial in red circle) . a) total evolution. b) 80-100ms evolution.

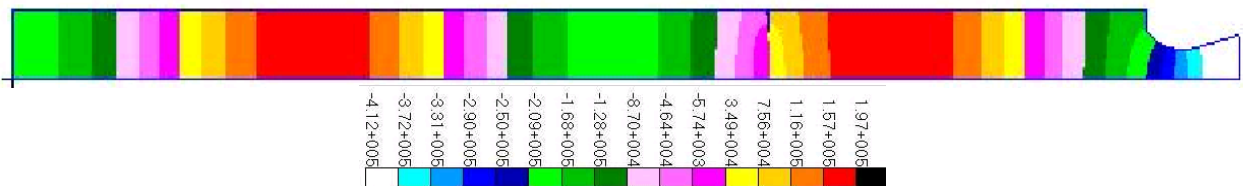


Figure 12 : 4L acoustic mode (MSC.Nastran Software).

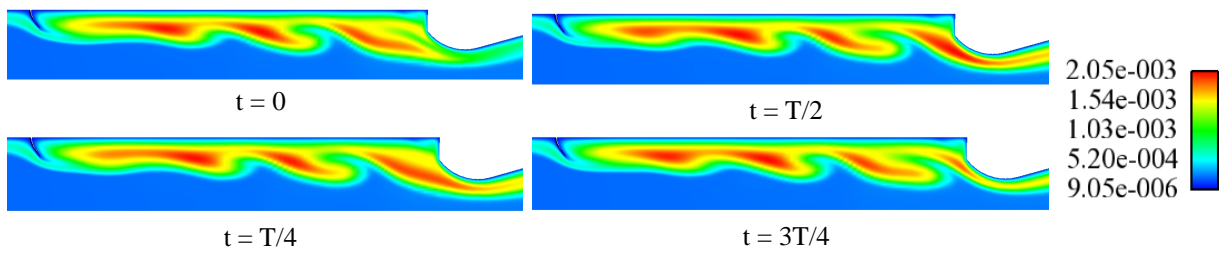


Figure 13 : Evolution of mixing length (m). Full period T represented.

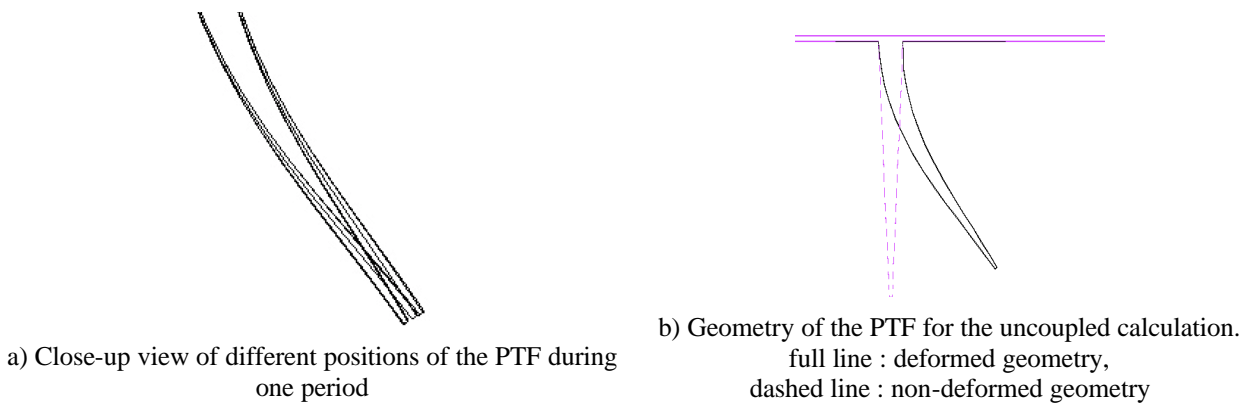


Figure 14 : Evolutions of the PTF obtained with the coupled calculation.

One notices a change in the main oscillations frequency and number of vortices lying between the obstacle and the nozzle when FSI phenomena are taken into account. The 2L acoustic mode observed in the uncoupled simulation shifts to the 4L mode when the PTF displacements are computed. At the moment, the origine of this frequency shift is still under investigation. It may be explained by the presence of a node pressure in the 4L mode shape, just at the position of the deformed inhibitor (Figure 12). Hence the maximum acoustic pressure gradient at that position in the 4L mode shape could be more likely to force the PTF to oscillate when its displacements are computed. To be more precise, in the coupled simulation, the PTF sustains a forced regime at the 4L frequency without any resonance between the structural eigenmodes and the acoustic ones. Indeed, a modal analysis of the PTF did not exhibit any eigenfrequencies around 1200 Hz.

## Conclusion

The coupling procedure developed by Snecma Propulsion Solide, SAFRAN Group jointly with ONERA and MSC.Software has been described and validated on an experimental configuration involving highly transient compressible phenomena. This constitutes a first step in the validation process of this coupling method that will be pursued in the future.

Then, a simplified small scale configuration of a segmented SRM has been computed. Even if this configuration is not fully representative of the transient regime of segmented SRMs, it enables us to assess the possible importance of FSI phenomena. One notices a frequency shift between the uncoupled and coupled simulations. The origine of this phenomenon is still under investigation and could be explained by the position of the inhibitor relatively to the acoustic mode shape. Hence it might be possible that FSI phenomena alter the flow acoustic coupling usually depicted as the triggering process of the instability in segmented SRMs.

A great challenging issue in the near future for Snecma Propulsion Solide, SAFRAN Group is to be able to compute the displacements inside a full scale SRM at a given operating point. Its real geometry is much more complicated than the one studied in this article. The good assessment of its deformation requires a more adequate fluid mesh deformation tool that should be available in the new unstructured ONERA code named CEDRE<sup>[16]</sup>. A great effort should also be made to take into account more realistic material laws for the inhibitor.

## Acknowledgements

The valuable comments of Dr. J. Giordano (IUSTI) on the work performed in section 2 are gratefully acknowledged. Our thanks also to J.-C. Tauzin, T. Mazuelas and F. Trouillez for their substantial contributions to this work.

## REFERENCES

- [1] Brown, R.S., Dunlap, R., Young, S.W. and Waugh, R.C., "Vortex shedding as a source of acoustic energy in segmented solid rockets," *Journal of Spacecraft*, 18(4), 312-319, 1981.
- [2] Dotson, K.W., Koshigoe, S. and Pace, K.K., "Vortex shedding in a large solid rocket motor without inhibitors at the segmented interfaces," *Journal of Propulsion and Power*, 13(2), 197-206, 1997.
- [3] Scippa, S., Pascal, P., and Zanier, F., "Ariane-5 MPS: Chamber pressure oscillations full scale firings results analysis and further studies," AIAA Paper 94-3068, 1994.
- [4] Lupoglazoff, N. and Vuillot, F., "Parietal Vortex Shedding as a Cause of Instability for Long Solid Propellant Motors. Numerical Simulations and Comparisons with Firing Tests", AIAA Paper 96-0761, 1996.
- [5] Giordano, J., Jourdan, G., Burtschell, Y., Medale, M., Zeitoun, D.E., and Houas, L. "Shock wave impacts on deforming panel, an application of fluid-structure interaction". *Shock Waves* (2005)
- [6] Farhat, C., Lesoinne, M., "Higher-Order Staggered and Subiteration Free Algorithms for coupled Dynamic Aeroelasticity Problems", 36th Aerospace Sciences Meeting and Exhibit, AIAA 98-0516, Reno/NV, 1998.
- [7] Dutoya, D. and Errera, M.P., "A Formal Decomposition of the Jacobian Matrix of the Euler Equations. Application To Upwind Numerical Schemes," *La Recherche Aérospatiale*, n° 1992-1, 1992
- [8] Scherrer, D. and Vuillot, F., "MSD/MSDH Applications," *1<sup>st</sup> ONERA-DLR Aerospace Symposium*, Paris 21-24 June 1999
- [9] Laroche, E., "Influence of freestream turbulence intensity on cooling effectiveness," ASME Paper 2001-GT-0139.
- [10] Hackenberg, M., Post, P., Redler, R., and Steckel, B., "MpCCI, Multidisciplinary Applications and Multigrid," Proceedings ECCOMAS 2000, CIMNE, Barcelona, 11-14 September 2000.
- [11] Ribéreau, D., Guery, J.-F. and Le Breton, P., "Numerical Simulation of Thrust Oscillations of Ariane 5 Solid Rocket Boosters", Space Solid Propulsion Conference, 2000.
- [12] Avalon, G. and Lambert, D., "Campagne d'essais VALDO. Période 2000/2001", », Technical Report, ONERA 2/05424 DEFA (2001).
- [13] Lesoinne, M., Farhat, C., "Geometric conservation laws for flow problems with moving boundaries and deformable meshes, and their impact on aeroelastic computations". *Comput. Meth. Appl. Mech. Eng.* 134,71-90 (1995)
- [14] Rockwell, D., "Oscillations of Impinging Shear Layers", *AIAA Journal*, Vol.21, No.5, p645-664, 1983.
- [15] Vuillot, F., "Programme ASSM – Méthodes d'ingénieur pour la prévision de la stabilité des moteurs à propergol solide », Technical Report, ONERA RT 73/6133EY (1996).
- [16] Chevalier, P, Courbet, B., Dutoya, D., Klotz, P., Ruiz, E., Troyes and J., Villedieu, P., "CEDRE, development and validation of a multiphysic computational software", EUCASS, Moscow, Russia, 2005.



**This page has been purposely left blank**